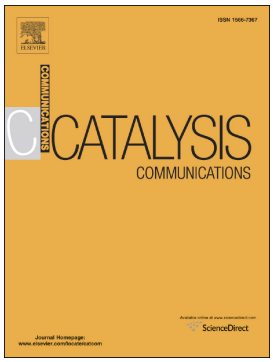


# Nickel oxide-silica core-shell catalyst for acetylene hydroxycarbonylation

Hong Sub Choi, Ji Hoon Park, Jong Wook Bae, Jin Hee Lee, Tae Sun Chang

PII: S1566-7367(19)30044-5
DOI: https://doi.org/10.1016/j.catcom.2019.02.009
Reference: CATCOM 5620

To appear in: *Catalysis Communications*

Received date: 9 November 2018
Revised date: 21 January 2019
Accepted date: 10 February 2019

Please cite this article as: H.S. Choi, J.H. Park, J.W. Bae, et al., Nickel oxide-silica core-shell catalyst for acetylene hydroxycarbonylation, Catalysis Communications, https://doi.org/10.1016/j.catcom.2019.02.009

# Nickel Oxide-Silica Core-Shell Catalyst for Acetylene Hydroxycarbonylation

Hong Sub Choi,[a,b] Ji Hoon Park,[a] Jong Wook Bae,[b] Jin Hee Lee,[a,*] Tae Sun Chang[a,*]

[a]Center for Environment & Sustainable Resources, Korea Research Institute of Chemical Technology, 141 Gajeong-ro, 34114 Daejeon, Republic of Korea.

[b]School of Chemical engineering, Sungkyunkwan University(SKKU), Suwon 16419, Republic of Korea

***Corresponding authors.** Fax: (+82)-042-860-7593, e-mail: leejh@krict.re.kr (J.H. Lee), tschang@krict.re.kr (T.S. Chang)



## Abstract

Acrylic acid and its ester derivatives are important chemicals utilized to synthesize numerous end products. Acrylic acid is industrially produced via propylene oxidation. We report in this study a nickel oxide-silica core-shell catalyst ($NiO@SiO_2$) for acetylene hydroxycarbonylation as an alternative way to synthesize acrylic acid. $NiO@SiO_2$ catalyst provided the higher turnover frequency and yield than commercial nickel oxide catalyst on acetylene

hydroxycarbonylation. The carbon monoxide/acetylene ratio influenced more significantly to initial reaction rate than final acrylic acid yield. The silica shell protected the nickel oxide from sintering during reaction, however, the catalyst was deactivated by coke formation, attributed to acetylene decomposition.

**Keywords**

Acetylene, Hydroxycarbonylation, Nickel oxide, Acrylic acid, Core-shell, Sintering process.

## 1. Introduction

Acrylic acid (AA) is the simplest unsaturated carboxylic acid, which vinyl group is directly connected to carboxylic acid functionality. AA and its ester derivatives are transformed to numerous functional polymer materials via self-polymerization and/or co-polymerization with acrylamide, acrylonitrile, styrene, and butadiene etc [1-5]. The resulting materials are utilized to manufacture a variety of products such as textile, plastic, adhesive, coating, and elastomer [6].

AA is mainly produced by oxidation of propylene originated from petroleum. Although the propylene oxidation is well established, new synthetic routes that reduce the use of petroleum derived chemicals are required to withstand an increasing oil-price. Acetylene hydroxycarbonylation is a plausible

alternative to synthesize AA (acetylene + CO + $H_2O$ → acrylic acid)[7-10]. Reppe first reported the acetylene hydroxycarbonylation in 1939 using nickel tetracarbonyl ($Ni(CO)_4$) as a catalyst [11]. However, the high toxicity of nickel tetracarbonyl limited the commercial application. Other nickel catalysts have, thus, been developed to replace nickel tetracarbonyl. Tang et al. synthesized AA with high yield and selectivity using nickel acetate [12]. Hao Xie and co-workers reported the use of heterogeneous nickel oxide in acetylene hydroxycarbonylation [13]. The nickel oxide supported on MCM-41 resulted the highest yield and turnover frequency (TOF). Lin et al. studied the effects of the nickel oxide preparation method in acetylene hydroxycarbonylation activity [14].

In this study, we employed a nickel oxide coated with porous silica shell ($NiO@SiO_2$) as a catalyst for acetylene hydroxycarbonylation. The silica shell inhibits the leaching and aggregation of active nickel oxide nanoparticles while allowing diffusion of the reactants and the product. The effects of numerous reaction parameters on the AA yield and reaction rates are examined.

## 2. Experimental

### 2.1 Materials

Carbon monoxide (99.95%) was purchased from Bingrae gases Co., Ltd

and acetylene (97%) was purchased from Sinchun gas. Nickel nitrate hexahydrate ($Ni(NO_3)_2 \cdot 6H_2O$), polyethylene glycol (MW20000) were purchased from Alfa aesar. Pluronic P123 (Poly(ethylene glycol)-block-poly(propylene glycol)-block-Poly(ethylene glycol)-block), Polyvinylpyrrolidone (PVP, MW40000), ammonium hydroxide solution (28%), tetraethyl orthosilicate (TEOS, 98%), mesitylene (98%), ammonium fluoride ($NH_4F$, 98%), hydrochloric acid (HCl, 35-37%) were purchased from Sigma Aldrich. Sodium hydroxide, ethanol (95%), acetone (95%) were purchased from Samchun Chemical. All the chemicals were used without purification.

### 2.2 Catalyst synthesis

The $NiO@SiO_2$ was synthesized by a slight modification of reported procedure [15]. Nickel nitrate hexahydrate (2.9 g) was dissolved in distilled water (40 mL, and the solution was stirred at room temperature for 30 min. The solution was added dropwise to the mixture of distilled water (100 mL), polyethylene glycol (330 mg), and sodium hydroxide (1.0 g). The resulting mixture was stirred at room temperature for 1 h, then filtered and washed using distilled water and ethanol. The mixture was dried at 50 °C for 24 h and calcined at 350 °C for 2 h to give the nickel oxide nanoparticles. 100 ml of an ethanolic solution containing PVP (0.10 g) and nickel oxide nanoparticles (0.20 g) was stirred for 12 h at room temperature. 25% aqueous ammonia solution (10

ml) was added into the solution and sonicated for 30 min. The ethanol solution (5.0 mL) containing TEOS (0.10 mL) was added and stirred for 1 h. The resulting suspension was washed by centrifugation for three times using ethanol and distilled water. The precipitate was collected and dried at 80 °C for 6 h to give 0.21 g of NiO@$SiO_2$.

For the synthesis of NiO/$SiO_2$, the mesoporous silica was prepared by reported procedure [16]. Pluronic P123 (16 g) was dissolved in 1.6 M aqueous HCl solution (150 mL). Mesitylene (4.0 g) and $NH_4F$ (0.046 g) were added to the solution and stirred at room temperature for 1 h. TEOS (8.8 g) was added, and the mixture was stirred at 40 $^oC$ for 24 h. The resulting suspension was filtered with water and the obtained solid was dried for 24 h at 100 $^oC$. Calcination for 8 h at 500 $^oC$ gave the mesoporous silica. The nickel nitrate hexahydrate (0.33 g dissolved in 2.0 mL distilled water) aqueous solution was impregnated to the mesoporous silica (1.0 g) and dried at 80 °C. The resulting solid was calcined at 400 °C for 3 h to give NiO/$SiO_2$.



**2.3 Catalyst characterization**

The crystal structure of catalysts was characterized by X-ray diffraction (XRD, Bruker) using Cu Kα radiation (λ=1.5406 Å) at 40 kV and 100 mA. The scan was performed in the 2 $^o min^{-1}$ range of 10 ° to 80 ° with 0.02 °$step^{-1}$, and 1

s•step$^{-1}$. For transmission electron microscopy (TEM) measurement, the material was dispersed in ethanol and a few drops were deposited onto a copper grid. TEM was performed on a Talos F20S (FEI Talos) at an acceleration potential of 200 kV. The thermogravimetric analysis (TGA) was implemented on a TGA Q5000 (TA). The 2.3290 g of analyte was loaded on a platinum microcrucible and heated up to 700 °C at a ramping rate of 10 °Cmin$^{-1}$ under an air flow of 25 mL•min$^{-1}$. Chemisorption were performed with ASAP 2020 (Micromeritics) at 35 °C using 99.999% hydrogen. Before analysis, the samples were reduced at 450 °C under 99.999% hydrogen for 4 h followed by evacuation at 450 °C.

**2.4 Catalytic reaction.**

The catalytic acetylene hydroxycarbonylation was performed in a 100 mL autoclave made of stainless steel. In a typical experiment, 12.9 mg of NiO@$SiO_2$ (3.78 $mM_{Ni}$), 10 mg of copper (II) bromide (1.12 $mM_{Cu}$) were added to the 40 mL mixture of distilled water and acetone (acetone/water = 1:9 volume ratio) The reactor was purged with argon and charged to 3 bar with acetylene followed by pressurizing with CO up to 30 bar at 28 °C. The amounts of introduced gas were monitored by mass flow controller. The reaction mixture was heated to 220 °C while stirring at 300 rpm. The reaction temperature and pressure were recorded automatically. After the reaction, the reactor was quickly

cooled under 50 °C and purged with Ar. The reaction mixture were collected and evaporated to remove residual acetone. The AA yield was determined by $^{1}$H nuclear magnetic resonance (NMR) spectroscopy using ethanol as an internal standard. For the quantification of AA, 30 mmol of ethanol was added to the reaction mixture before $^{1}$H NMR analysis. The amount of AA was calculated based on the integration ratio of C*H*3 proton of ethanol and C*H* proton of AA. The AA yield and initial TOF of the reaction was calculated by following equations. Identical mole concentration of nickel and copper were used for other catalysts.

$$\text{amounts of AA (mmol)} = \frac{integration\ value\ of\ CH\ proton\ of\ AA}{intgration\ value\ of\ CH3\ proton\ of\ ethanol} \times 30\ (mmol) \quad (1)$$

$$\text{AA yield (\%)} = \frac{\text{amounts of AA determined by } {}^{1}H\text{ NMR}}{\text{amounts of acetylene measured by MFC}} \times 100 \quad (2)$$

$$\text{TOF } (h^{-1}) = \left(\frac{pressrue\ drop\ at\ inital\ 5\ min}{total\ pressure\ drop}\right) \times \text{produced AA (mmol)} \times \frac{1}{surface\ Ni\ (mmol)} \times \frac{60}{5} \quad (3)$$

## 3. Results and Discussion

Nickel oxide nanoparticles were prepared by precipitation using polyethylene glycol as a stabilizer. The formation of 8.8 ± 4.1 nm nickel oxide

nanoparticles were confirmed by TEM analysis (Figure 1a). The silica shell was introduced on the surface of nickel oxide to cover and isolate nickel oxide nanoparticles by modified Stober's method. PVP was employed to give porous structure to the silica shell. The formation of 8.5 ± 4.1 nm nickel oxide nanoparticles enclosed by 5.1 ± 2.2 nm silica shell were found in the TEM images (Figure 1b). The nickel oxide nanoparticles maintained the original size during the silica shell formation. The TEM image showed the most of the nickel oxide nanoparticles were isolated from other particles by silica. The nitrogen isotherm plot of NiO@$SiO_2$ showed the type II isotherm which had a hysteresis in the $P/P_0$ range of 0.4-0.9. This result indicates the mesoporous nature of NiO@$SiO_2$ (Figure S1a). The XRD patterns of nickel oxide and NiO@$SiO_2$ exhibited a typical nickel (II) oxide structure (Figure S1b). No peaks correspond to silica were observed due to amorphous nature of the silica shell.

Acetylene hydroxycarbonylation was performed to test the catalytic activity of nickel catalysts. Nickel bromide produced 22% of AA and the yield was improved to 47% in presence of copper bromide (Table 1, entries 1, 2). The copper has known to promote the AA production by enhancing carbon monoxide solubility [12]. Commercial nickel oxide exhibited poor AA yield due to low metallic surface area (Table 1, entry 3). Both NiO/$SiO_2$ and NiO@$SiO_2$ showed comparable AA yield to nickel bromide (Table 1, entries 5, 6). However, specific activity of NiO@$SiO_2$ was higher than NiO/$SiO_2$ as confirmed by TOF.

This result signifies that the surface active sites on NiO@$SiO_2$ are more active toward acetylene hydroxycarbonylation than NiO/$SiO_2$. When the copper oxide was employed instead of copper bromide, the reaction did not proceed with both NiO and NiO@$SiO_2$.

The effect of carbon monoxide/acetylene molar ratios on the AA yield and formation rate was investigated (Figure 2). The carbon monoxide/acetylene ratios were adjusted by varying initial acetylene pressure. AA yield increased as carbon monoxide/acetylene ratio increased from 0.6 to 0.9, then kept similar yields between carbon monoxide/ acetylene ratios of 0.9-1.5. The AA yield decreased over carbon monoxide/acetylene ratio of 1.5. However, the TOFs followed a volcano curve, which had a peak value at the carbon monoxide/acetylene ratios of 1.3-1.1. Because the solubility of carbon monoxide is low, high carbon monoxide concentration increases the initial reaction rate. Whereas, too high carbon monoxide concentration might increase the surface coverage of carbon monoxide on nickel oxide, and retards AA formation by inhibition of the acetylene coordination onto catalyst surface. In contrast to TOF, the highest AA yield was achieved in the broad range of carbon monoxide/acetylene ratio (1.5-0.9) regardless of initial reaction rate. Figure S2 shows the time on stream pressure changes of three reactions, which were carbon monoxide/acetylene ratio of 1.5, 1.1, 0.9. In all the cases, the pressure rapidly drops initially then, the decrease rates were slow down. The initial

reaction rates were affected by carbon monoxide/acetylene ratios and the order was 1.1 > 0.9 > 1.5. Although initial AA formation rates were different, the reactions further proceeded for 3 h and resulted in the identical AA yields on three different reactions (Figures 2 and S2).

AA formation rates were influenced by reaction conditions, such as ratios of reactant, and catalyst. However, final AA yields were not significantly affected to the varying initial reaction rates. The results implicate that acetylene hydroxycarbonylation stops at certain conversion level due to inhibition of high AA concentration in the reaction mixture. Thus, controlled amounts of AA were added to reactor to investigate possible effects of AA on the acetylene hydroxycarbonylation. Figure 3 clearly shows the negative effects of additional AA to acetylene hydroxycarbonylation. Both initial reaction rates and final AA quantities were reduced when AA was added. Because acetylene hydroxycarbonylation is irreversible in our reaction condition, the retardation of AA formation is not due to the reaction equilibrium but attributes to inhibition of the catalytic cycle. Based on the previous reports of nickel and palladium catalyzed hydroxycarbonylation, nickel oxide catalyzed acetylene hydroxycarbonylation mechanism is proposed (Figure 4) [12, 17]. Copper (II) bromide initially oxidized to copper (I) bromide by acetylene and produce hydrogen bromide [18]. The catalytic cycle starts from hydroxylation of nickel oxide by hydrogen bromide. The copper (I) forms copper-acetylene pi

complex[19] to facilitate the adsorption of acetylene onto the nickel oxide. The proton is transferred to the acetylene to form nickel-vinyl complex with simultaneous nickel oxidation [17]. Following carbon monoxide insertion and bromide assisted hydroxylation produce AA. Because produced AA competitively coordinates onto nickel surface against acetylene and carbon monoxide, excess AA likely hinders the catalytic cycle and decrease the reaction rate. In addition, increased acidity of reaction medium prevents the formation of AA and results in the low yield.

The reusability of the NiO@$SiO_2$ was tested. The catalyst was recovered by centrifugation and reused without a specific treatment. As shown in Figure S3, the catalyst was deactivated in the three times of reuse. TEM images of the reused catalyst showed that the catalyst maintained the core-shell structure without significant aggregation (Figure 5). The particle size of the used NiO@$SiO_2$ was 8.4 nm. While, the particle size of the non-protected nickel oxide was grown from 7.1 nm to 12.4 nm (Figure S4). Although the nickel oxide nanoparticles were stable, substantial amounts of fiber-like carbon which had a thickness of 31 ± 10 nm was observed on used NiO@$SiO_2$. TGA revealed 12 wt% of carbon was contained in the spent catalyst (Figure S5). In addition, nickel oxide was not leached out during the reaction as determined by inductively coupled plasma (ICP) analysis of reaction mixture. Although the nickel oxide was stable, the coke formation by acetylene decomposition

influenced the durability of the catalyst. As reported by other nickel oxide catalyst system, carbon product can be removed by oxidation process and possibly recover catalytic activity [6, 13, 14].

## 4. Conclusions

In conclusion, we synthesized a NiO@$SiO_2$ core-shell catalyst for acetylene hydroxycarbonylation. The core-shell catalyst provided higher acrylic acid yield and TOF than commercial nickel (II) oxide and mesoporous silica supported nickel oxide. The optimum CO/acetylene ratio was critical to achieve high TOF while final AA yield was less sensitive to CO/acetylene ratio. The core-shell structure successfully protected the nickel oxide from sintering but coke formation by acetylene decomposition caused catalyst deactivation. The AA itself hinders the acetylene hydroxycarbonylation by binding onto the active catalyst surface, thus the reaction cannot proceed to completion in current catalytic system. The reaction system that prevents the inhibiting roles of AA and/or the catalyst that resists to AA coordination are needed to achieve higher AA yield.



## Acknowledgements

This research was supported by KRICT Steppingstone Program for SMEs R&D, Korea Research Institute of Chemical Technology (KRICT).

**References**

[1] I.-T. Trotuş, T. Zimmermann, F. Schüth, Catalytic Reactions of Acetylene: A Feedstock for the Chemical Industry Revisited, Chem. Rev., 114 (2014) 1761-1782. https://doi.org/10.1021/cr400357r

[2] H. Xie, D. Yi, L. Shi, X. Meng, High performance of CuY zeolite for catalyzing acetylene carbonylation and the effect of copper valence states on catalyst, Chem. Eng. J., 313 (2017) 663-670. https://doi.org/10.1016/j.cej.2016.11.043

[3] J. Hou, M.-L. Yuan, J.-H. Xie, Q.-L. Zhou, Nickel-catalyzed hydrocarboxylation of alkynes with formic acid, Green Chem., 18 (2016) 2981-2984. https://doi.org/10.1039/C6GC00549G

[4] T.J. Lin, H. Xie, X. Meng, L. Shi, Characterization and catalytic application of Bi2O3/NiO composite oxides in the Reppe carbonylation to acrylic acid, Catal. Commun., 68 (2015) 88-92. https://doi.org/10.1016/j.catcom.2015.04.032

[5] T.-j. Lin, X. Meng, L. Shi, Activity and Sediments Study for the Hydrocarboxylation of Acetylene with Carbon Monoxide to Acrylic Acid on

Ni–Cu Homogeneous Catalyst, Ind. Eng. Chem. Res., 52 (2013) 14125-14132. https://doi.org/10.1021/ie4021446

[6] T.J. Lin, X. Meng, L. Shi, Ni-exchanged Y-zeolite: An efficient heterogeneous catalyst for acetylene hydrocarboxylation, Appl. Catal. A-Gen., 485 (2014) 163-171. https://doi.org/10.1016/j.apcata.2014.07.036

[7] H. Schobert, Production of Acetylene and Acetylene-based Chemicals from Coal, Chem. Rev., 114 (2014) 1743-1760. https://doi.org/10.1021/cr400276u

[8] S. Quintero-Duque, K.M. Dyballa, I. Fleischer, Metal-catalyzed carbonylation of alkynes: key aspects and recent development, Tetrahedron Lett., 56 (2015) 2634-2650. https://doi.org/10.1016/j.tetlet.2015.04.043

[9] F. De Angelis, A. Sgamellotti, N. Re, Density Functional Study of the Reppe Carbonylation of Acetylene, Organometallics, 19 (2000) 4104-4116. https://doi.org/10.1021/om0002428

[10] G. Kiss, Palladium-catalyzed Reppe carbonylation, Chem. Rev., 101 (2001) 3435-3456. https://doi.org/10.1021/cr010328q

[11] W. Reppe, H. Kröper, Carbonylierung II. Carbonsäuren und ihre Derivate aus olefinischen Verbindungen und Kohlenoxyd, Liebigs. Ann. Chem., 582 (1953) 38-71. https://doi.org/10.1002/jlac.19535820103

[12] C. Tang, Y. Zeng, P. Cao, X. Yang, G. Wang, The Nickel and Copper-Catalyzed Hydroformylation of Acetylene with Carbon Monoxide to Acrylic Acid, Catalysis Lette., 129 (2009) 189-193. https://doi.org/10.1007/s10562-008-

9789-6

[13] H. Xie, T. Lin, L. Shi, X. Meng, Acetylene carbonylation over Ni-containing catalysts: role of surface structure and active site distribution, RSC Adv., 6 (2016) 97285-97292. https://doi.org/10.1039/C6RA17567H

[14] T.J. Lin, X. Meng, L. Shi, Catalytic hydrocarboxylation of acetylene to acrylic acid using Ni2O3 and cupric bromide as combined catalysts, J. Mol. Catal. A-Chem., 396 (2015) 77-83. https://doi.org/10.1016/j.molcata.2014.09.027

[15] L. Li, S. He, Y. Song, J. Zhao, W. Ji, C.-T. Au, Fine-tunable Ni@porous silica core–shell nanocatalysts: Synthesis, characterization, and catalytic properties in partial oxidation of methane to syngas, J. Catal., 288 (2012) 54-64. https://doi.org/10.1016/j.jcat.2012.01.004

[16] L. Wolski, I. Sobczak, M. Ziolek, Development of multifunctional gold, copper, zinc, niobium containing MCF catalysts – Surface properties and activity in methanol oxidation, Micropor. Mesopor. Mat., 243 (2017) 339-350. https://doi.org/10.1016/j.micromeso.2017.02.038

[17] L. Crawford, D.J. Cole-Hamilton, E. Drent, M. Buhl, Mechanism of alkyne alkoxycarbonylation at a Pd catalyst with P,N hemilabile ligands: a density functional study, Chem., 20 (2014) 13923-13926. https://doi.org/10.1002/chem.201403983

[18] G. Zhang, H. Yi, G. Zhang, Y. Deng, R. Bai, H. Zhang, J.T. Miller, A.J.

Kropf, E.E. Bunel, A. Lei, Direct Observation of Reduction of Cu(II) to Cu(I) by Terminal Alkynes, J. Am. Chem. Soc., 136 (2014) 924-926. https://doi.org/10.1021/ja410756b

[19] B.T. Worrell, J.A. Malik, V.V. Fokin, Direct Evidence of a Dinuclear Copper Intermediate in Cu(I)-Catalyzed Azide-Alkyne Cycloadditions, Science, 340 (2013) 457-460. https://doi.org/10.1126/science.1229506

**Table 1**. Catalytic activity comparison of various nickel catalyst[a)]

**Figure 1**. TEM images of (a) NiO and (b) $NiO@SiO_2$. Scale bars are 10 nm.

**Figure 2**. Effects of carbon monoxide/acetylene ratios on $NiO@SiO_2$ catalyzed acetylene hydroxycarbonylation.

**Figure 3**. Effects of AA addition on $NiO@SiO_2$ catalyzed acetylene hydroxycarbonylation.

**Figure 4**. Proposed reaction mechanism and inhibition by AA.

**Figure 5**. TEM images of reused $NiO@SiO_2$. Scale bars are 100 nm.

**Table 1**. Catalytic activity comparison of various nickel catalyst[a)]

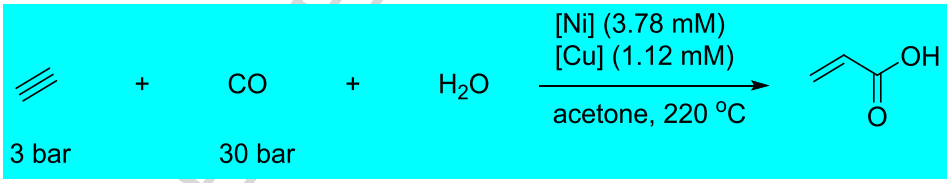


| Entry | Ni | Cu | AA yield (%)[b)] | TOF[c)] ($x10^6$) |
|---|---|---|---|---|
| 1 | $NiBr_2$ | | 22 | 0.036 |
| 2 | $NiBr_2$ | $CuBr_2$ | 47 | 0.040 |
| 3 | NiO | $CuBr_2$ | 14 | 15 |
| 4 | NiO | CuO | - | - |

| | | | | |
|---|---|---|---|---|
| 5 | $NiO/SiO_2$ | $CuBr_2$ | 48 | 0.99 |
| 6 | $NiO@SiO_2$ | $CuBr_2$ | 48 | 15 |
| 7 | $NiO@SiO_2$ | CuO | - | - |

a) The 3.78 mM of nickel and 1.12 mM of copper were added to the 1:9 mixture of water/acetone mixture. Then, 3 bar of acetylene and 30 bar of carbon monoxide were charged. The temperature of the reactor was increased to 220 °C and kept for 4 h. b) Determined by $^1H$ NMR using ethanol as an internal standard. c) Calculated based on the amounts of surface nickel oxide determined by $H_2$-chemisorption.



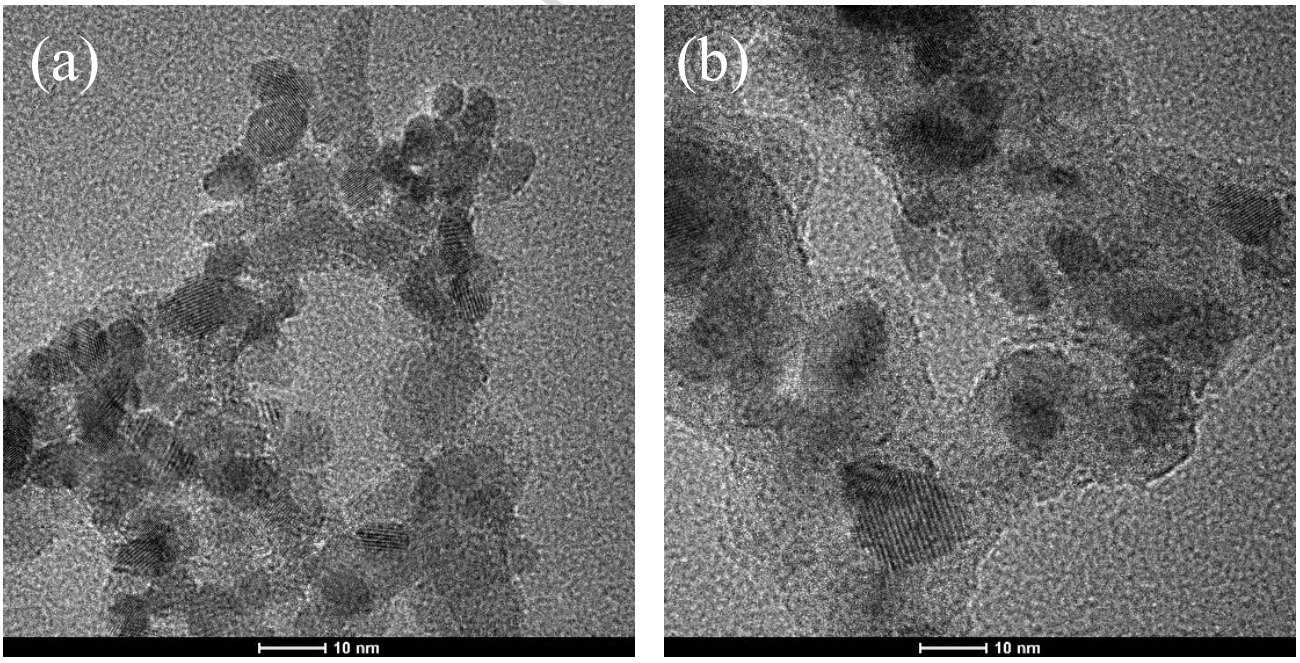


**Figure 1**. TEM images of (a) NiO and (b) $NiO@SiO_2$. Scale bars are 10 nm.

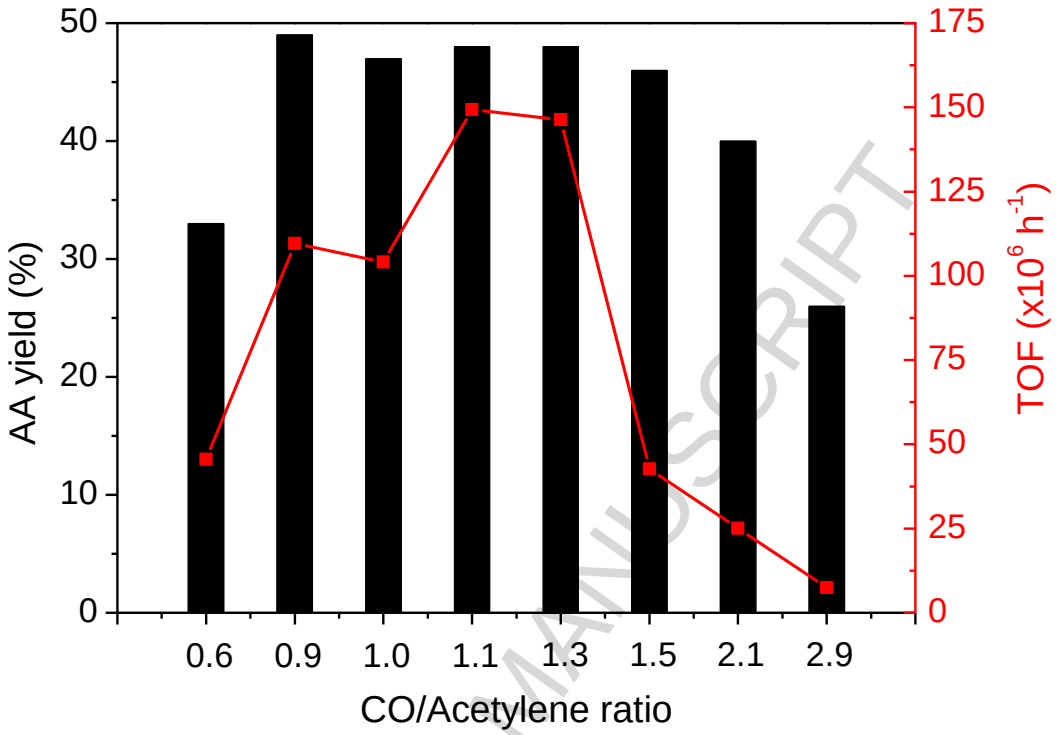


**Figure 2**. Effects of carbon monoxide/acetylene ratios on NiO@$SiO_2$ catalyzed acetylene hydroxycarbonylation.

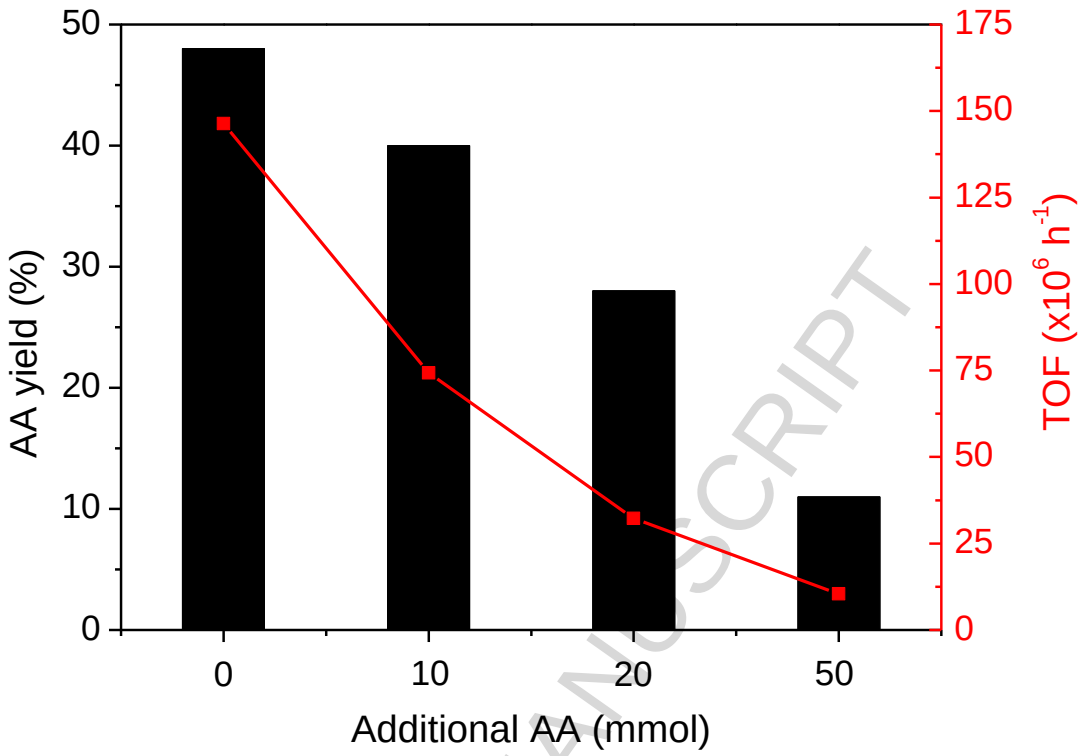


**Figure 3**. Effects of AA addition on $NiO@SiO_2$ catalyzed acetylene hydroxycarbonylation.

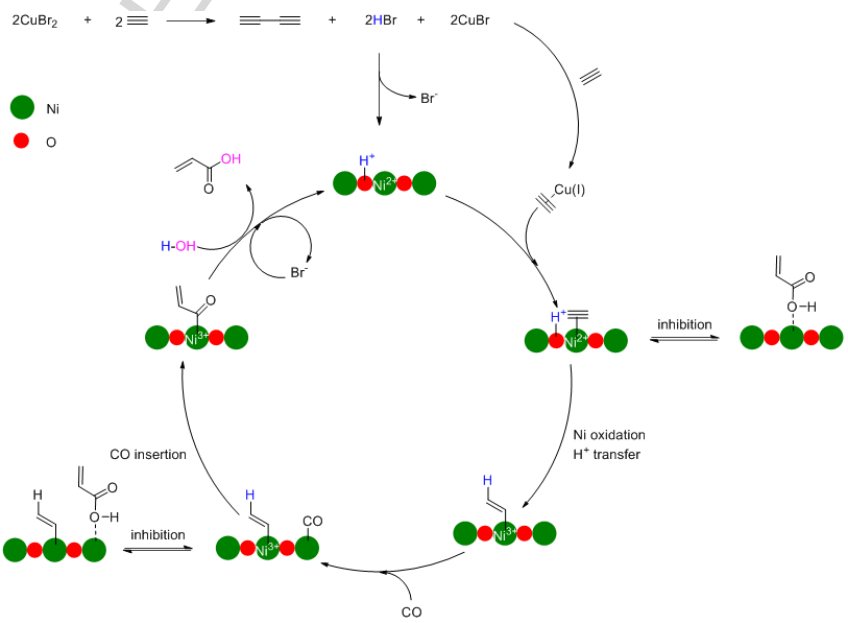

**Figure 4**. Proposed reaction mechanism and inhibition by AA.

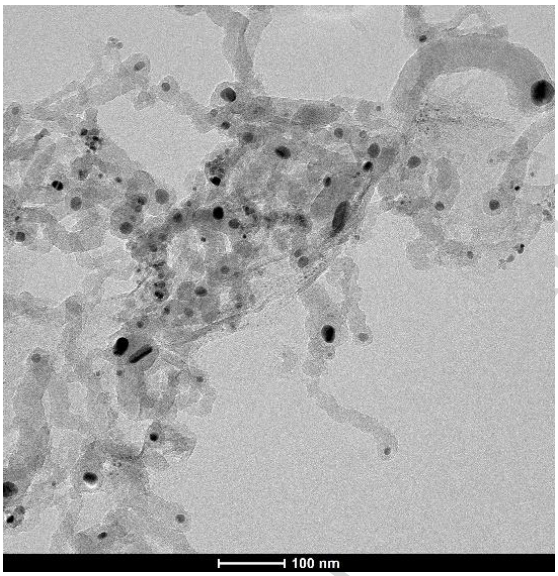


**Figure 5**. TEM images of reused $NiO@SiO_2$. Scale bar is 100 nm.



## Highlights

- The $NiO@SiO_2$ core-shell catalyst provided higher acrylic acid yield and turnover frequency.
- The core-shell structure protected the nickel oxide from sintering.
- The acrylic acid itself inhibits the catalytic cycle by binding onto the active sites.
- Formation of coke by acetylene decomposition leads to deactivation of catalyst.

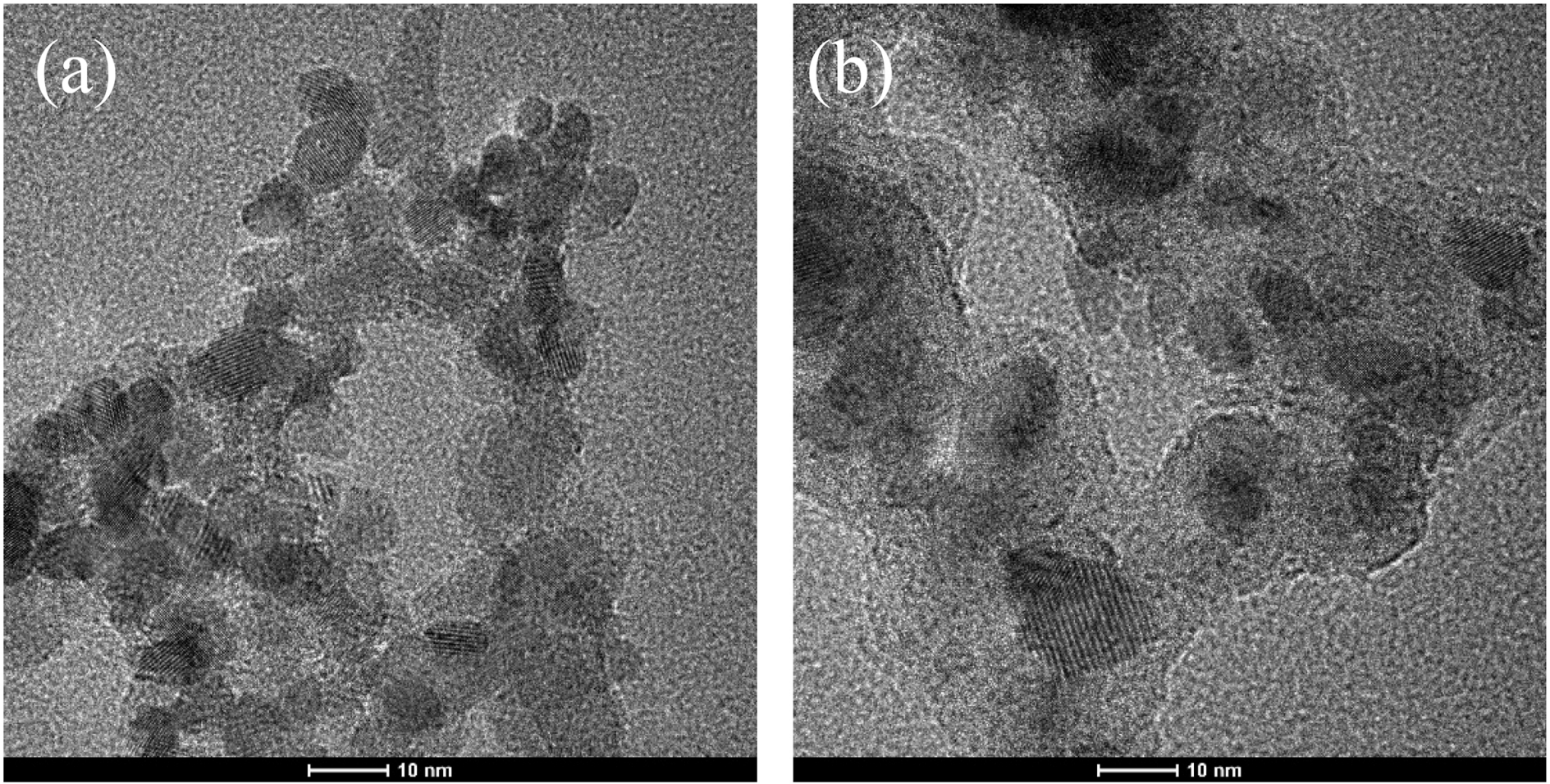


Figure 1

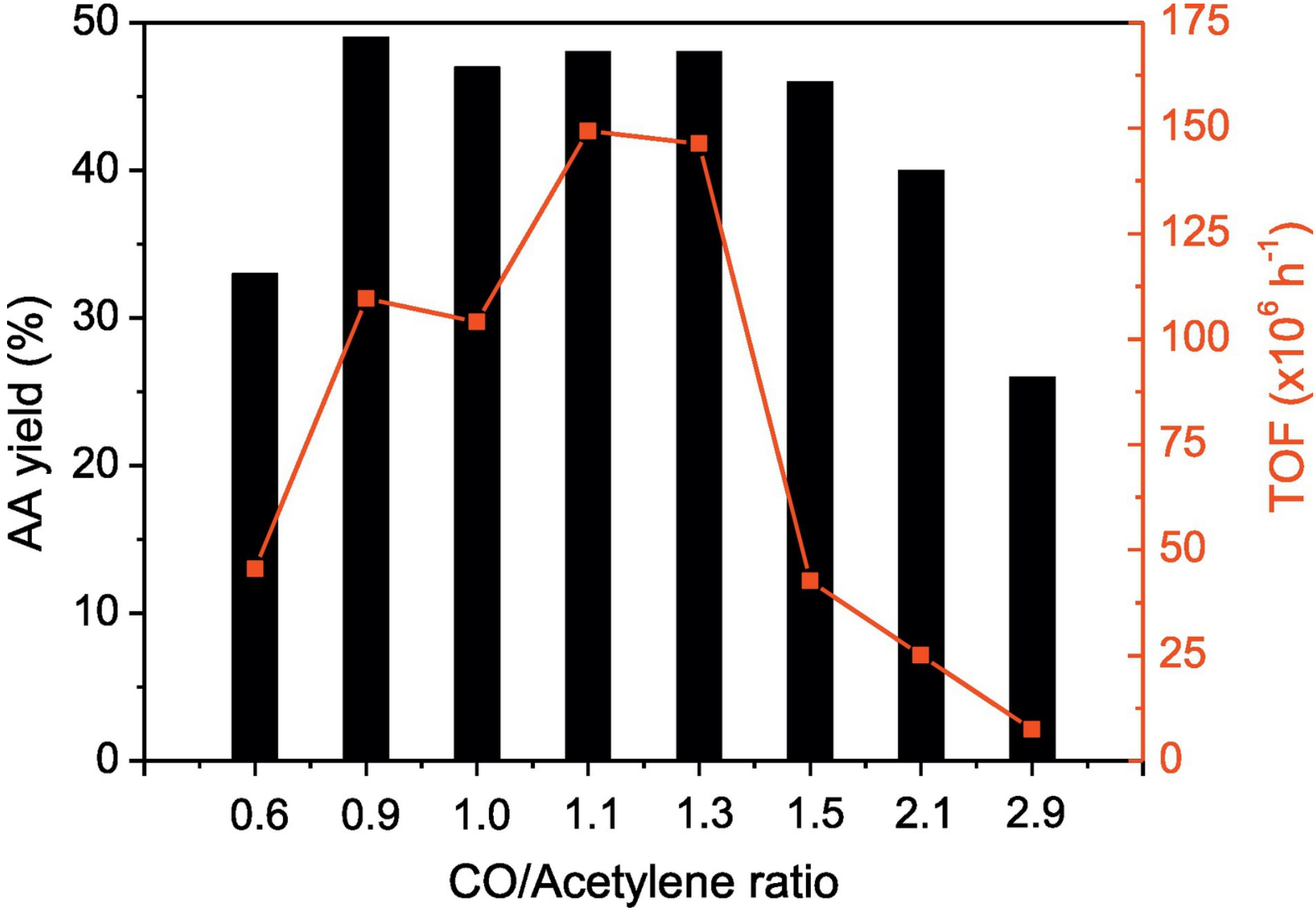
AA yield (%)
TOF (x10^6 h^-1)
CO/Acetylene ratio
0
10
20
30
40
50
0
25
50
75
100
125
150
175
0.6
0.9
1.0
1.1
1.3
1.5
2.1
2.9

Figure 2

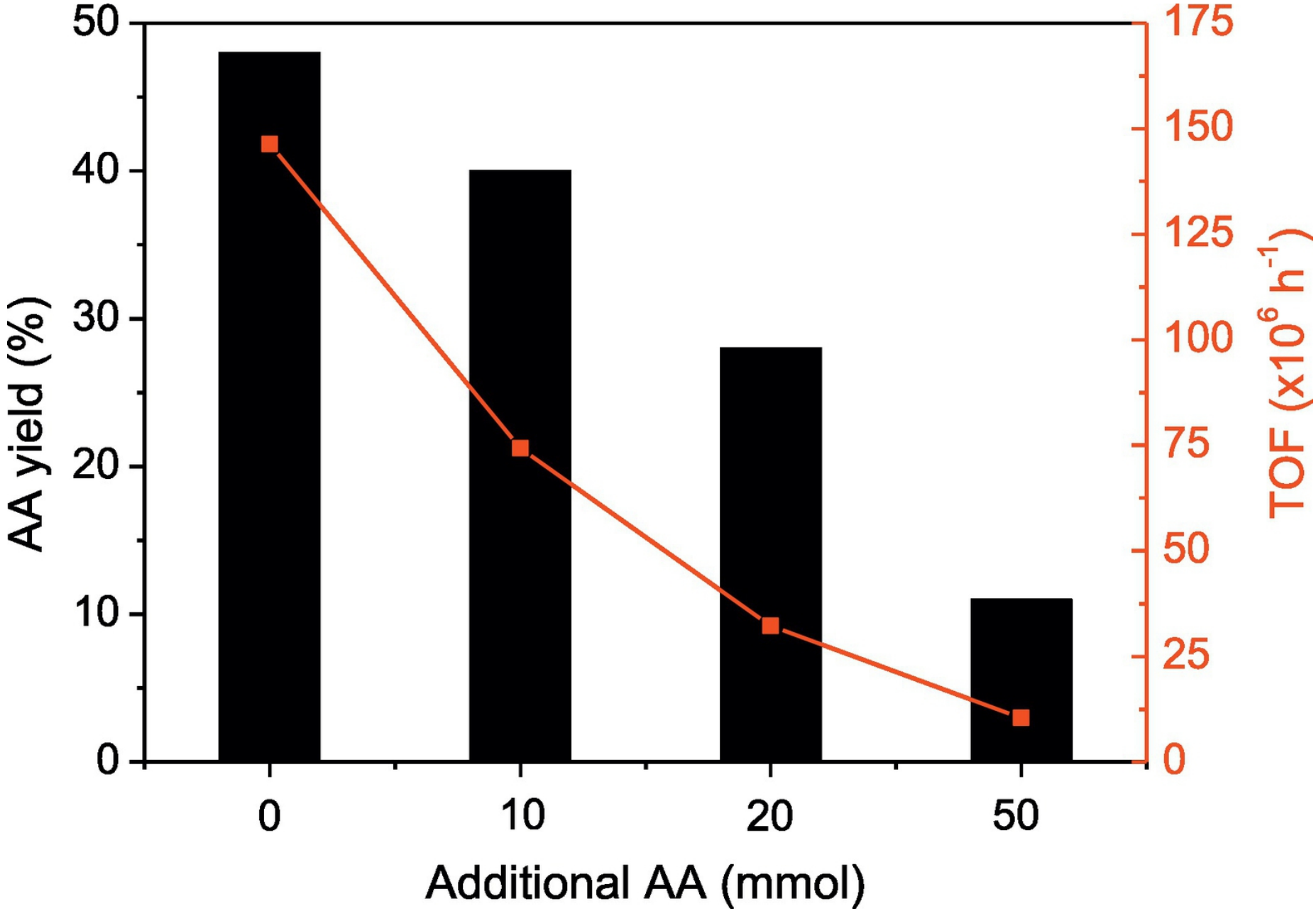
AA yield (%)
TOF (x10^6 h^-1)
Additional AA (mmol)
0
10
20
30
40
50
0
25
50
75
100
125
150
175
0
10
20
50

Figure 3

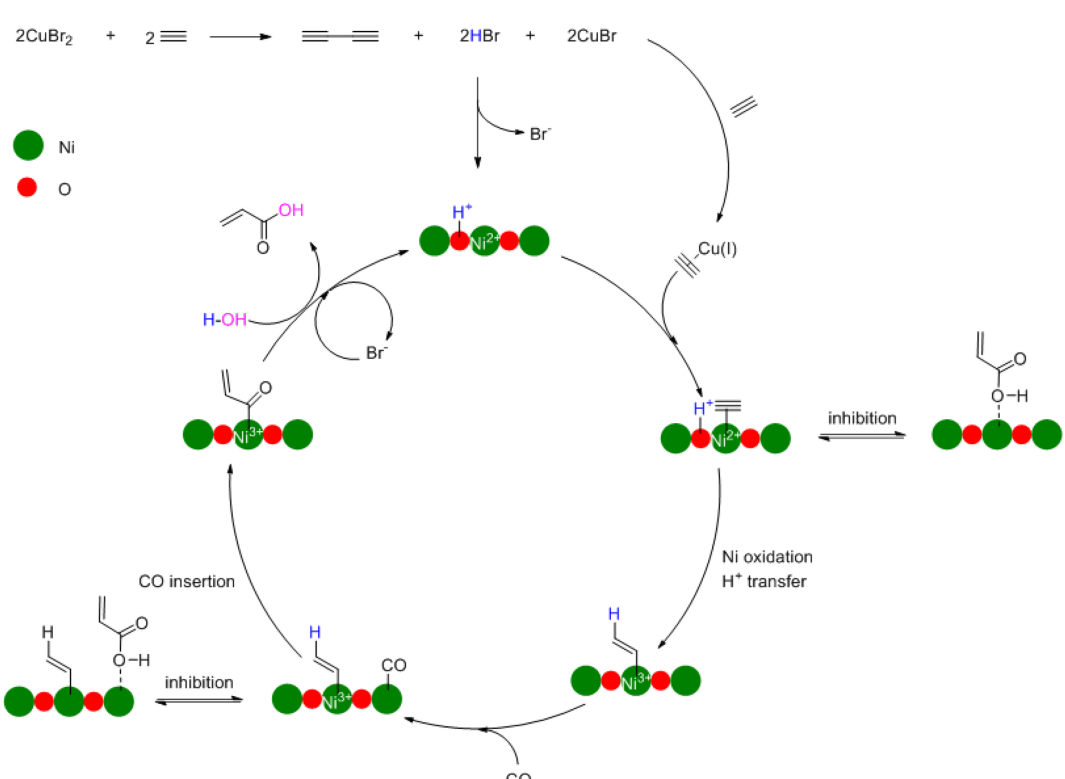
2CuBr2 + 2 + 2HBr + 2CuBr
Br-
Ni
O
OH
O
H+
Ni2+
Cu(I)
H-OH
Br-
Ni3+
H+
Ni2+
inhibition
O
O–H
Ni oxidation
H+ transfer
H
Ni3+
CO
CO insertion
H
O
O–H
inhibition
H
Ni3+
CO

Figure 4

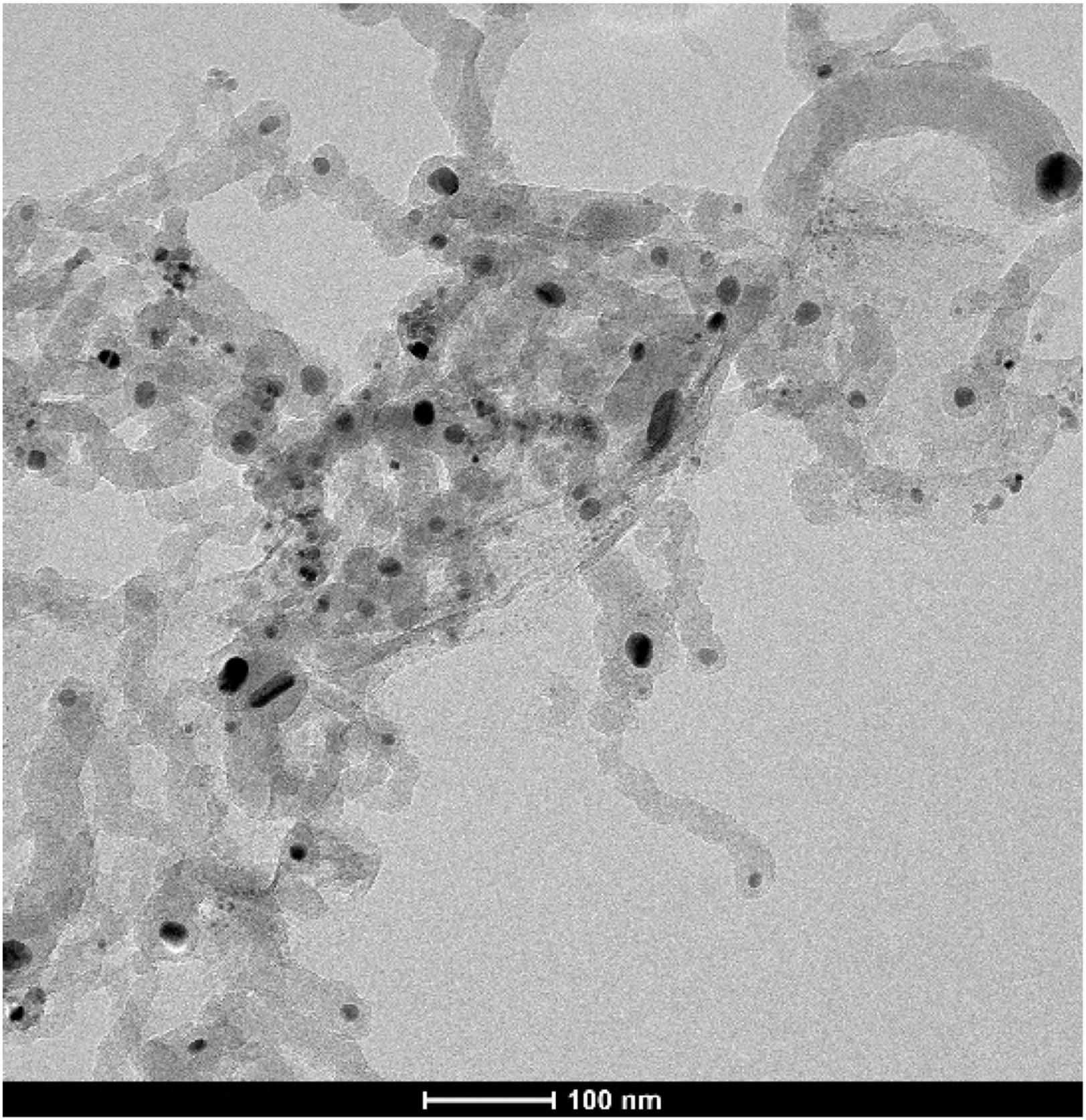


Figure 5